On the Parameterization of Hermite Transform with Application to the Compression of QRS Complexes

Miloš Brajović[1], Irena Orović, Miloš Daković, Srdjan Stanković

University of Montenegro/Electrical Engineering Department
20 000, Podgorica, Montenegro
phone: + (382) 69 486 639, fax: + (382) 20 245 873

Abstract

The concentration and sparsity of signal representation in the Hermite transform (HT) basis may highly depend on a properly chosen scaling factor and discrete time shift parameter. In that sense, we propose a simple and efficient iterative procedure for automatic determination of the optimal scaling factor. The optimization criterion is based on the ℓ_1-norm acting as a measure of signal concentration in the HT domain. Instead of centering the signal at the zero time instant, we also propose to shift the center for a few points left or right, which will additionally improve the concentration. An important application of the proposed optimization approach is the compression of QRS complexes, where properly chosen scaling factor and time-shift increase the compression performance. The results are verified using synthetic and real examples and compared with the existing approach for the compression of QRS complexes.

Keywords: Concentration measures, Gradient algorithm, ECG signal, Hermite function, Hermite transform, QRS complex

1. Introduction

The Hermite transform (HT) has been studied during the last few decades, particularly as an alternative to the Fourier transform [[1]-[16]]. Although covering a wide range of possible applications due to many interesting properties, Hermite transform has been extensively used for the representation of QRS complexes, especially for their compression, as well as feature evaluation and extraction [[1]-[9],[11]]. Other applications include: molecular biology [[8]], image processing and computed tomography [[8],[9],[11]], radar signal processing [[12]], physical

[1]Corresponding author
Email: milosb@ac.me, phone: +38269486639 (Miloš Brajović)

optics [[13]] etc.

QRS complexes, as the most characteristic waves of ECG signals, are important for medical diagnosis and treatments. In the processing and compression of ECG signals and QRS complexes, many authors applied different kinds of wavelets and corresponding transforms [[17]-[19]]. Recently, it was shown that the Hermite transform may provide far better performance, when it is appropriately optimized [[1]]. Namely, the Hermite transform is found to be a suitable mathematical tool for the representation of QRS complexes due to their similarity with Hermite functions (HF). In other words, these signals can be represented using a few Hermite coefficients [[1]-[7],[10]]. This property has been exploited in the development of several compression algorithms for QRS complexes [[5]-[7]], that established a theoretical framework, having a lack of practical applications due to use of continuous domain functions [[1]]. An algorithm that proposes the use of discrete Hermite functions is presented in [[1],[2]]. Hence, we start from the HT based algorithm [[1],[2]], which significantly outperforms the compression based on other transforms, such as DFT, DCT and DWT, in the applications with ECG signals. This approach uses an experimentally obtained value of the scaling factor, which “stretches” and “compresses” the QRS complex to match the orthogonal basis. Herein, we employ a concentration measure based algorithm to get optimal HF parameters [20]. It leads to better performance of approach proposed in [[1],[2]]. The idea arises from the currently attractive area of compressive sensing and sparse signal reconstruction [[14]-[22]]. Hence, an iterative procedure for the determination of the optimal scaling factor and time-shift is proposed leading to the improved compression performance, as verified on real ECG signals database [[23]].

The paper is organized as follows. In Section 2, an overview of the discrete HT calculation for uniformly sampled signals is provided. The optimization of the spread factor and time-shift parameter is proposed in Section 3. Section 4 presents the numerical results, while the concluding remarks are given in Section 5.

2. The Hermite transform

2.1. Discrete Hermite transform

Hermite polynomial of the p-th order, widely known among the orthogonal polynomials, can be defined as [[1]-[14], [24]]:

$$H_p(t) = (-1)^p e^{t^2} \frac{d^p(e^{-t^2})}{dt^p}. \tag{1}$$

The p-th order HF is related with p-th order Hermite polynomial as follows:

$$\psi_p(t,\sigma)=\left(\sigma 2^p p!\sqrt{\pi}\right)^{-1/2} e^{-\frac{t^2}{2\sigma^2}} H_p(t/\sigma), \tag{2}$$

where the scaling factor σ is introduced to "stretch" and "compress" HF, in order to better match the signal [[1]-[10]]. The Hermite expansion is defined as [[1]-[14]]:

$$f(t)=\sum_{p=0}^{\infty} c_p \psi_p(t,\sigma), \tag{3}$$

where c_p denotes the p-th order Hermite coefficient:

$$c_p=\int_{-\infty}^{\infty} f(t)\psi_p(t,\sigma)dt,\ p=0,1,\ ...,\ M-1. \tag{4}$$

For the numerical calculation of the integral (4) the Gauss-Hermite quadrature approximation [[1]-[8],[14]]:

$$c_p=\frac{1}{M}\sum_{m=1}^{M}\frac{\psi_p(t_m,\sigma)}{\left[\psi_{M-1}(t_m,\sigma)\right]^2} f(t_m),\ \ p=0,1,...,M-1, \tag{5}$$

is commonly used, where t_m denotes the zeros of the M-th order Hermite polynomial (1). As it is discussed in the literature [[1], [24], 25], there is no closed-form expression for the roots of the Hermite polynomials. Also, some examples of the roots for the first 10 Hermite polynomials are given in [[14]].

In general, for the case of continuous-time signals, an infinite number of Hermite functions is needed for the representation of the signal without approximation errors in (3), [[1]]. In the discrete case, it is assumed that discrete HF and analyzed signals are obtained by sampling their continuous counterparts at non-equispaced sampling points associated with the roots of Hermite polynomials [[1],[2],[4],[13]]. Namely, in that case any discrete signal of length M can be uniquely represented by the expansion of exactly M discrete Hermite functions in (3), i.e., this signal representation is complete, [[1]].

The time axis scaling factor σ is used to "stretch" and "compress" HF relatively to the analyzed signal $f(t)$. As proposed in [[1],[2]], we can alternatively fix σ = 1 and introduce an equivalent parameter λ to "stretch" and "compress" the signal $f(t)$ relatively to the HF basis.

The inverse and direct HT, (3) and (5) can be written in matrix-vector notation. Let us introduce the HT matrix as:

$$\mathbf{W}_H = \frac{1}{M}\begin{bmatrix} \frac{\psi_0(t_1,1)}{\psi_{M-1}^2(t_1,1)} & \frac{\psi_0(t_2,1)}{\psi_{M-1}^2(t_2,1)} & \cdots & \frac{\psi_0(t_M,1)}{\psi_{M-1}^2(t_M,1)} \\ \frac{\psi_1(t_1,1)}{\psi_{M-1}^2(t_1,1)} & \frac{\psi_1(t_2,1)}{\psi_{M-1}^2(t_2,1)} & \cdots & \frac{\psi_1(t_M,1)}{\psi_{M-1}^2(t_M,1)} \\ \vdots & \vdots & \ddots & \vdots \\ \frac{\psi_{M-1}(t_1,1)}{\psi_{M-1}^2(t_1,1)} & \frac{\psi_{M-1}(t_2,1)}{\psi_{M-1}^2(t_2,1)} & \cdots & \frac{\psi_{M-1}(t_M,1)}{\psi_{M-1}^2(t_M,1)} \end{bmatrix}_{M\times M}. \tag{6}$$

If we introduce the vector of Hermite coefficients $\mathbf{c} = [c_0, c_1, \ldots, c_{M-1}]^T$ and $\hat{\mathbf{f}} = [f(\lambda t_1), f(\lambda t_2), \ldots, f(\lambda t_M)]^T$ vector with M signal samples at the points proportional to the roots of the M-th order Hermite polynomial, λt_1, λt_2,…, λt_M, according to Gauss-Hermite quadrature formula (5) the HT can be written as:

$$\mathbf{c} = \mathbf{W}_H \hat{\mathbf{f}}. \tag{7}$$

Having in mind the expansion (3), the inverse transform matrix is:

$$\mathbf{W}_H^{-1} = \begin{bmatrix} \psi_0(t_1,1) & \psi_1(t_1,1) & \cdots & \psi_{M-1}(t_1,1) \\ \psi_0(t_2,1) & \psi_1(t_2,1) & \cdots & \psi_{M-1}(t_2,1) \\ \vdots & \vdots & \ddots & \vdots \\ \psi_0(t_M,1) & \psi_1(t_M,1) & \cdots & \psi_{M-1}(t_M,1) \end{bmatrix}.$$

Based on the previous matrix definitions, the inverse HT for the case of discrete signals reads:

$$\hat{\mathbf{f}} = \mathbf{W}_H^{-1}\mathbf{c}. \tag{8}$$

2.2. *Hermite transform of uniformly sampled signals*

Consider a continuous-time signal $f(t)$ with compact support, such that $f(t) = 0$ for $t \notin [-T, T]$, sampled uniformly to obtain the corresponding finite duration discrete-time signal $f(n)$, of odd-length $M = 2K+1$, $n = -K,\ldots, K$, with Δt being the sampling period. According to the sampling theorem, the continuous-time signal can be reconstructed and resampled at the desired points λt_1, λt_2,…, λt_M according to:

$$f(\lambda t_m) \approx \sum_{n=-K}^{K} f(n\Delta t)\frac{\sin\left(\pi(\lambda t_m - n\Delta t)/\Delta t\right)}{\pi(\lambda t_m - n\Delta t)/\Delta t}, \tag{9}$$

where $m = 1,\ldots, M$, $n = -K,\ldots, K$, or in matrix form:

$$\hat{\mathbf{f}} \approx \mathbf{A}_\lambda \mathbf{f}, \tag{10}$$

with $\hat{\mathbf{f}}$ being the vector containing values of signal sampled at the desired points $t=\lambda t_m$, corresponding to zeros of the M-th order Hermite polynomial (1) and **f** is the vector of original signal samples taken uniformly according to the sampling theorem. In the case of even-length signal $M = 2K$, in (9) values $n = -K,\dots, K-1$ are assumed.

In the expanded form, (10) can be written as:

$$\begin{bmatrix} f(\lambda t_1) \\ f(\lambda t_2) \\ \vdots \\ f(\lambda t_M) \end{bmatrix} \approx \begin{bmatrix} a_{11} & a_{12} & \cdots & a_{1M} \\ a_{21} & a_{22} & \cdots & a_{2M} \\ \vdots & \vdots & \ddots & \vdots \\ a_{M1} & a_{M2} & \cdots & a_{MM} \end{bmatrix} \begin{bmatrix} f(-K) \\ f(-K+1) \\ \vdots \\ f(K) \end{bmatrix}, \tag{11}$$

where $M = 2K + 1$ and elements a_{ij} being defined with:

$$a_{ij} = \sin\left[\pi(\lambda t_i - (j-K-1)\Delta t)/\Delta t\right] / \left[\pi(\lambda t_i - (j-K-1)\Delta t)/\Delta t\right],$$

with $i, j \in \{1, 2, \dots, M\}$. As recently presented in [[26]], the truncation error [27] using sinc interpolation is largest for time instants near the edges of the grid. However, in the case of compact time-support signals, the truncation error will be negligible even at the edges (e.g., -50dB for signal given in Example 1). Furthermore, the problem of interpolation of finite signals is also discussed from the perspective of FIR filter-based sinc interpolation in [27], where it is emphasized that the truncation effects could be alleviated by multiplying the interpolation kernel $\sin\left(\pi(t-n\Delta t)/\Delta t\right)/(\pi(t-n\Delta t)/\Delta t)$ with a window function.

The uniformly sampled signal and the corresponding HT now can be related by combining (7) and (11) as:

$$\mathbf{c} = \mathbf{W}_H \hat{\mathbf{f}} \approx \mathbf{W}_H \mathbf{A}_\lambda \mathbf{f}. \tag{12}$$

3. Parameter optimization

3.1. Scaling factor

In this Section, we propose to employ the concentration measure of the Hermite coefficients vector **c** to calculate the suitable value of λ, which will allow to represent the signal with most concentrated (or even the sparsest) Hermite transform vector **c**. It is important to emphasize that the criterion is defined such that the classical uniform sampling of signals is assumed, without need for new sampling devices. The concentration measures, such as the ℓ_1-norm of transform coefficients, have been used in optimizations where it is crucial to concentrate a signal transform in a small number of coefficients [[4],[20]-[22]]. One of the most recent applications is in the compressed sensing. The ℓ_1-norm of the HT can be calculated as:

$$\mathcal{M} = \left\|\mathbf{c}\right\|_1 = \sum_{p=0}^{M-1}\left|c_p\right|. \tag{13}$$

Thus, the optimal value of λ is obtained by solving:

$$\lambda = \arg\min_{\lambda}\left\|\mathbf{c}\right\|_1 = \arg\min_{\lambda}\left\|\mathbf{W}_H\mathbf{A}_\lambda\mathbf{f}\right\|_1. \tag{14}$$

Note that (14) is a 1D search problem over the possible range of λ values. Thus, one can perform the search over the range of possible values of λ, finding the one that minimizes the concentration measure. This range can be determined such that the roots of the Hermite polynomial are mainly placed between the existing sampling points, as discussed in [[1]].

The basic idea behind the proposed algorithm is to iteratively search for the optimal value λ, starting from a predefined value $\lambda^{(0)}$. In each iteration k, a small value Δ is added and subtracted from the current λ, to determine the change of concentration measure. Then, $\lambda^{(k)}$ is updated by a value which decreases the measure (13) in a steepest descent manner. Similar approach was employed to reconstruct missing samples of sparse signals [[4],[21]]. The algorithm is given as follows:

Algorithm 1. Calculation of the optimal scaling factor λ

Require:

- Signal vector $\mathbf{f}$ of length $M = 2K + 1$
- Step parameter μ
- Transform matrix $\mathbf{W}_H$, calculated according to (6)

1: Set $\lambda^{(0)} \leftarrow M\Delta t / \left[2\left(\sqrt{\pi(M-1)/1.7}+1.8\right)\right]$

2: Set $\Delta \leftarrow 2/t_M$

3: Set $\varepsilon \leftarrow 10^{-10}$

While $\Delta > \varepsilon$

4: $\mathbf{A}_\lambda^{+} \leftarrow \begin{bmatrix} a_{11}^{+} & a_{12}^{+} & \cdots & a_{1M}^{+} \\ a_{12}^{+} & a_{22}^{+} & \cdots & a_{2M}^{+} \\ \vdots & \vdots & \ddots & \vdots \\ a_{M1}^{+} & a_{M2}^{+} & \cdots & a_{MM}^{+} \end{bmatrix}, \mathbf{A}_\lambda^{-} \leftarrow \begin{bmatrix} a_{11}^{-} & a_{12}^{-} & \cdots & a_{1M}^{-} \\ a_{12}^{-} & a_{22}^{-} & \cdots & a_{2M}^{-} \\ \vdots & \vdots & \ddots & \vdots \\ a_{M1}^{-} & a_{M2}^{-} & \cdots & a_{MM}^{-} \end{bmatrix}$

$$a_{ij}^{\pm} = \frac{\sin\left[\pi\left((\lambda\pm\Delta)t_i-(j-K-1)\Delta t\right)/\Delta t\right]}{\pi\left((\lambda\pm\Delta)t_i-(j-K-1)\Delta t\right)/\Delta t},\ i, j \in \{1, 2, \dots, M\}$$

5: $\mathcal{M}^{+} \leftarrow \left\|\mathbf{c}^{+}\right\|_1 = \sum_{p=0}^{M-1}\left|\mathbf{W}_H\mathbf{A}_\lambda^{+}\mathbf{f}\right|, \mathcal{M}^{-} \leftarrow \left\|\mathbf{c}^{-}\right\|_1 = \sum_{p=0}^{M-1}\left|\mathbf{W}_H\mathbf{A}_\lambda^{-}\mathbf{f}\right|$

6: $\nabla^{(k)} \leftarrow \left(\mathcal{M}^{+} - \mathcal{M}^{-}\right)/M$

7. $\lambda^{(k+1)} \leftarrow \lambda^{(k)} - \mu\nabla^{(k)}$

8: $\beta \leftarrow \operatorname{sign}\left(\nabla^{(k)}\nabla^{(k-1)}\right)$

9: **If** $\beta < 0$ **then** $\Delta \leftarrow \Delta/2$

End while

10: **Return** $\lambda^{(k)}$

Here, $\lambda^{(0)} = M\Delta t/\left[2(\sqrt{\pi(M-1)/1.7}+1.8)\right]$ is used as the starting point, which is the lower bound for the scaling factor defined in [[15],[16]] in order to ensure the convergence of the algorithm. The values of μ and Δ are chosen to provide optimal results for all considered signals. A too small step μ leads to slow convergence, while on the other side μ should be as small as possible to keep the algorithm stable (i.e., to ensure that the upper bound $\lambda < \left[\sqrt{\pi M/1.7}+1.8\right]/\left[2\pi W\right]$ is satisfied [[15],[16]], with W being the frequency bandwidth). Hence, the value of μ is set up empirically as a trade-off between these two requirements.

Maximal number of iterations corresponds to the signal length (in the experiments, the convergence is obtained even for number of iterations equal to the half of the signal length). The computational complexity of the algorithm can be approximated as follows (one iteration is considered): a) to generate the argument of the sinc function in Step 4, we need $2M^2+2$ additions (or subtractions) and $6M^2$ multiplications with constants; b) the interpolation is done with M^2 multiplications and $M(M-1)$ additions; c) For the two HT calculations, the complexity is $2M^2$ additions and $2M^2$ multiplications; d) the concentration measures requires $2M-2$ additions. Hence, the proposed algorithm requires $5M^2+M$ additions and $9M^2$ multiplications in total.

Two-dimensional (2D) Hermite transform can be obtained by calculating one-dimensional Hermite transforms separately in both directions [14]. Hence, the proposed approach can be easily generalized in a straight-forward manner for the case of 2D signals.

3.2. *Shift parameter*

The basis functions can be also shifted left or right along the time axis [[10]]. Instead of centering the signal at the zero time instant [[1],[2]], here we propose to shift center for a few sampling points left or right, before the calculation of the coefficients. In other words, instead of $f(n\Delta t)$, we use: $f_m(n\Delta t) = f((n \pm l)\Delta t)$ in (9), with

$l = [-l_{\max}, l_{\max}]$.

For every discrete shift value l, optimal λ is calculated in order to minimize (14). The measure vector $\mathbf{L}$ is formed containing the minimal measure value (14) obtained for the optimal λ, for every considered l. We find the l corresponding to the minimal value of $\mathbf{L}$, solving:

$$l = \arg\min_{l} \mathbf{L} \tag{15}$$

Note that $l_{\max}$ has a small value, e.g. $l_{\max} = 3$ for the case of QRS complexes, and thus a direct search in (15) is applied. The integer shift values are used in this paper, since the fractional shifts may require an additional interpolation which causes difficulties in the minimization of the concentration measure [[10]].

4. Numerical results

***Example 1*:** Let us observe the signal of the form:

$$f(t) = -3\sin(5\pi t)\exp\left(-\frac{(Mt)^2}{2\sigma_0^2}\right) \tag{16}$$

with $M = 61$, $\sigma_0 = 1.25$, $-1/2 < t < 1/2$, sampled with $\Delta t = 1/M$ to obtain discrete values at the uniform grid $n = -(M-1)/2, \ldots, (M-1)/2$. Original signal with uniformly sampled points and the corresponding Hermite coefficients with $\sigma = 1$ are shown on Fig. 1 (a) and (b) respectively. Note that the signal is characterized by the compact time support and it has the similar shape as the Hermite basis functions. Hence, these types of signals (windowed or low-pass filtered sinusoids, QRS segments, short-duration signals such as FHDSS, or UWB signals) are amenable to the proposed approach.

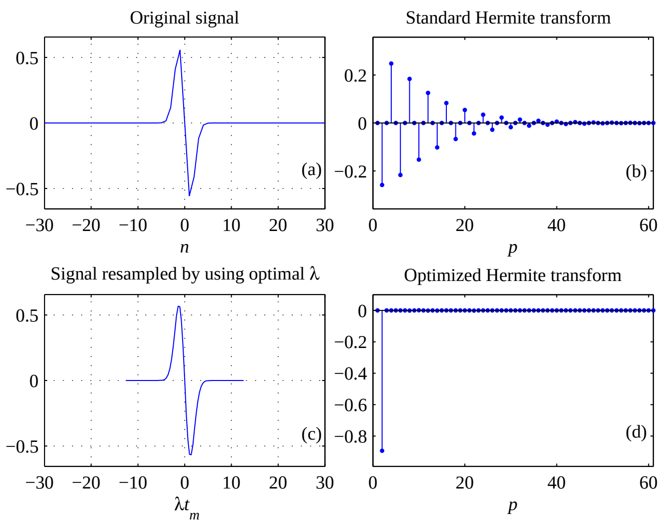

Fig. 1. Scaling factor influence on the HT: (a) original signal (16) and (b) the corresponding Hermite coefficients; (c) optimally scaled signal resampled at the roots of Hermite polynomial, and (d) Hermite coefficients of resampled signal

The proposed iterative procedure has been applied in order to find the most concentrated HT of the resampled signal. The obtained result is $\lambda = \sigma_0 \Delta t = 1.25 / M$ since we have intentionally incorporated the spread factor as the parameter of the Gaussian window in (16). The resampled signal with appropriately rescaled time axis, sampled at the roots of the *M*-th order Hermite polynomial, and corresponding Hermite coefficients are shown on Fig. 1 (c) and (d). We can observe that the optimal value of the scaling factor will assure that there is only one significant coefficient at $p = 2$, while other coefficients are close or equal to zero.

In order to check whether the proposed algorithm finds the optimal value, the concentration measure is calculated for different values of scaling factor λ: $1/\Delta t \le \lambda / \Delta t \le 2/\Delta t$, varied with the step $0.01/\Delta t$. The results are plotted in Fig. 2a, where the global minimum $\lambda_{\min} = 1.25/\Delta t$ is clearly visible on the curve.

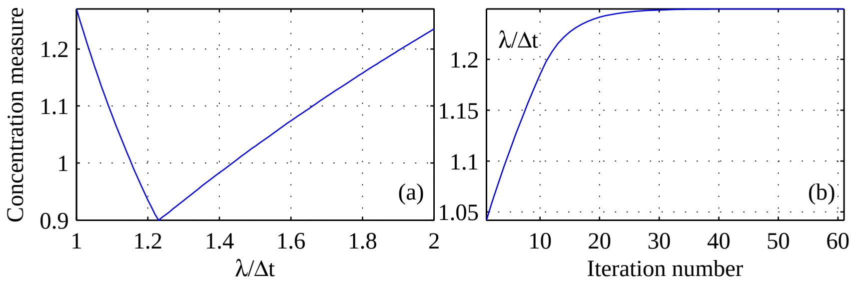

Fig. 2. a) The concentration measure in terms of $\lambda/\Delta t$, b) the learning curve of $\lambda/\Delta t$ through the iterations

Here, it is assumed that the lower and upper bounds of λ are satisfied [[15],[16]]. Lower bound is controlled by the algorithm initialization, and suitably chosen step μ assures that the upper bound is never reached. In this interval, a global minimum is expected to exist, corresponding to the most concentrated Hermite transform. Further, the learning curve of $\lambda/\Delta t$ with respect to iteration number is given in Fig. 2b. It can be observed that, as the algorithm reaches the minimum of the concentration measure, it stabilizes.

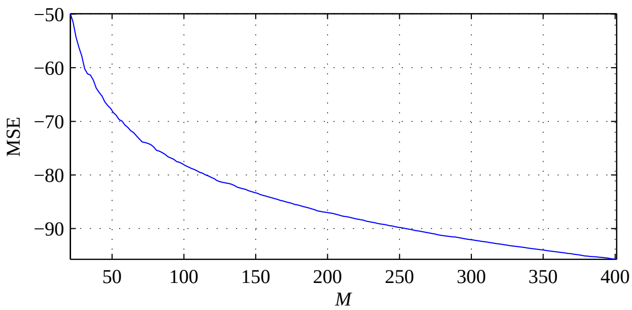

Fig. 3. MSE caused by the sinc interpolation kernel

The influence of truncation error introduced by the finite sinc kernel is also examined calculating the MSE between the interpolated signal $f_{\text{int}}(\lambda t_m)$ (interpolation is done based on uniform samples $f(n)$ and relation (10)) and the original (analytic) signal (16) observed at points $t = \lambda t_m$: $MSE = \frac{1}{M}\sum_{m=1}^{M} |f_{\text{int}}(\lambda t_m) - f(\lambda t_m)|^2$. Hence, the signal length M is varied from 21 to 401 samples (with step 2). The results are shown in Fig. 3 (logarithmic scale) showing that even the largest error caused by sinc interpolation is as small as -50dB.

***Example 2*:** In the framework of the considered compression problem, it is important to represent QRS complexes with the smallest possible number of coefficients, with a medically acceptable error. The compression algorithm proposed in [[1]] and [[2]] operates as follows. It is assumed that the ECG signal (i.e. QRS complex) $f(t)$ is sampled at points $\lambda t_1, \lambda t_2, \ldots, \lambda t_M$, to obtain the vector $\hat{\mathbf{f}}$. Then the HT coefficients $\mathbf{c}$ are calculated by (7). Further, the vector $\tilde{\mathbf{c}}$ is formed by keeping L largest coefficients in $\mathbf{c}$ and setting others to zero. The signal approximation can be obtained according to (8):

$$\tilde{\mathbf{f}} = \mathbf{W}_H^{-1}\tilde{\mathbf{c}}. \tag{17}$$

Here, we will refer to the algorithm presented in [[1],[2]] which can be further improved, by the proposed optimization of the scaling factor and time-shift. The continuous signal $f(t)$ was sampled at the points $\lambda t_1, \lambda t_2, \ldots, \lambda t_M$, where the scaling factor λ is chosen to obtain smallest number of coefficients in $\tilde{\mathbf{c}}$ under the condition that the relative reconstruction error:

$$E = \frac{\|\tilde{\mathbf{f}} - \mathbf{f}\|_2}{\|\mathbf{f}\|_2} \tag{18}$$

is below 10%, which is medically acceptable [[1],[2]]. However, several problems arise. To determine the optimal scaling factor λ, starting from the continuous ECG signals, sampling process needs to be repeated for every λ from a suitable range of possible values, which can be a technical problem for sampling devices. Then, the HT is calculated for every possible λ, and (18) is used to find the optimal λ such that $E \leq 10\%$. The other possibility is to use a fixed value of λ. However, it can be shown that improper λ leads to the larger number of Hermite coefficients in $\tilde{\mathbf{c}}$. Moreover, our experiments as well as those in [[1],[2]] show that each QRS complex has a different optimal value of λ, which means that the sampling device has to be continuously readjusted. On the other side, when dealing with the discrete QRS complexes in [[1]], the signal is resampled according to (11) and search for the optimal λ is done by measuring the compression ratio, which has to be maximized under the condition that $E \leq 10\%$. However, this approach is numerically exhausting, since both direct and inverse Hermite transform need to be calculated for each observed number of largest coefficients and for each λ.

In this paper, we propose to search for an optimal λ by minimizing the concentration measure, before the compression is done. The compression procedure is done as in [[1]], while the improvement is provided using the scaling factor optimization and the time-shift optimization based on concentration measure (14).

We have extracted Q = 1486 QRS complexes, from the first 10 seconds in the first leads of 168 ECG signals obtained from the MIT-BIH Compression Test Database [[23]]. The signals are uniformly sampled with $\Delta t = 1/250$. Three different signal lengths are used [1]: $2K+1 \in \{27, 29, 31\}$. The compression results are shown in Table I as the average number of coefficients (producing $E \leq$ 10%) and the average compression ratio: $\mathrm{ACR} = \sum_{i=0}^{Q}(2K_i+1)/\sum_{i=0}^{Q}L_i$, where L_i is the number of nonzero HT coefficients in the i-th complex producing $E \leq$ 10%, $2K_i+1$ is the length of the i-th QRS complex. The second column (as well as the third and the fourth) shows the result published in [[1]].

Table 1
Average number of coefficients and compression ratio for 10% approximation error

Comparison criterion	Proposed HT algorithm	HT based algorithm in [1]	DFT-based	DCT-based
Average number of coefficients	5.0	5.8	8.3	7.3
Average compression ratio	6.2	5.3	3.7	4.3

In the original approach [[1]] that uses a demanding search approach over all possible λ, and average number of 5.8 coefficients is needed for the proper reconstruction with $E \leq 10\%$. The proposed method (first column of Table I) shows further improvement, if the set of considered time-shifts is extended with $l_{\max} = 3$, $l \in \{-3, -2, -1, 0, 1, 2, 3\}$. Namely, when both the time-shift and scaling factor are optimized as proposed, the same error level is achieved even if only 5 coefficients are used, which means that the improvement over the original algorithm is about 13.8%. The average value of the scaling factor over all Q = 1486 QRS complexes is $\lambda/\Delta t = 4.2495$ (in seconds $\lambda = 4.2495/250 = 0.017$, which is the value experimentally obtained in [[2]], thus confirming the accuracy of the proposed approach). The step $\mu = 0.05$ is used in the experiment.

Let us consider the estimate of average number of bits per sample: a) for the time domain we have 9 bps, b) in the case of optimized HT, there are 5 most important real-valued coefficients out of 31 within QRS complex (one zero value may appear between 5 nonzero coefficients, and 6 coefficients are count to be encoded), which results in the rate 2 bps; c) in the case of DFT, there are approximately 8 most important coefficients (with real and imaginary parts) to be encoded out of 31, which is approximately 7 bps in average.

An example of the analyzed QRS complexes from the database [[23]] is shown in Fig. 4. Original signal is shown on Fig 4. (a), with the Hermite coefficients in Fig 4. (b). The concentration measure is lowest for the time-shift l = 1, with the corresponding optimal scaling factor $\lambda/\Delta t = 0.4352$ (in seconds $\lambda = 0.0176$). The optimally shifted signal resampled at the roots of Hermite polynomial (with M = 27 and $\lambda/\Delta t = 0.4352$) is shown in Fig 4. (c), with the Hermite coefficients given in Fig. 4 (d). The reconstructed signal is given by dash-dotted line in Fig. 4. (c).

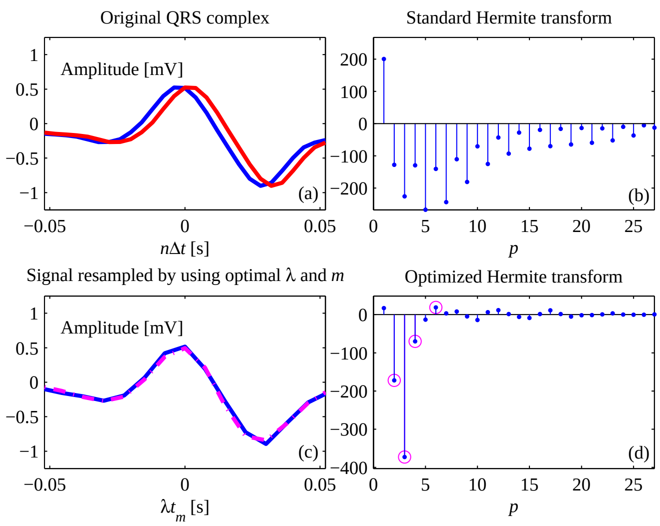

Fig. 4. Optimal scaling, shifting and resampling of QRS complex: (a) original signal (blue) and its shifted version (red); (b) Hermite coefficients of the original signal (standard Hermite transform); (c) shifted resampled signal with the optimal scaling factor (solid line) and reconstructed signal using largest 4 Hermite coefficients (relative error < 10%); (d) Optimized Hermite transform of rescaled and resampled signal (circles denote largest 4 coefficients)

Example 3: It is interesting to emphasize that the same approach can be applied to other types of signals such as the T waves of ECG signals, but also to the commonly present UWB signals (known as Gaussian doublets). Transmitting common Gaussian pulses directly to the antennas results in filtered pulses modeled as a derivative operation producing [[29]-[31]]: $s(t) = \left[1 - 4\pi\left(t/\tau_m\right)^2\right] e^{-2\pi\left(t/\tau_m\right)^2}$. A discrete version of this signal is considered, sampled at 2GHz, of length 100 ns and with $\tau_m = 22.2$ ns. The results of applying the proposed method on the ECG

T waves are shown in Fig. 5a. After applying the proposed algorithm, the observed part of ECG signal can be represented with only 14 coefficients out of 106 (13%), assuring the relative error (18) smaller than 10%. The average number of coefficients for the entire MIT-BIH Compression Test Database (first leads, first 10 seconds of 168 ECG signals) [23] is approximately 23% of the total length. In the case of UWB signals, the algorithm shows a high level of efficiency, providing a compact support with only 2 significant coefficients (Fig. 5b). Hence, in the context of UWB signals, the proposed approach has a potential in the design of UWB receivers, allowing the signals to be easily detected at the receiver.

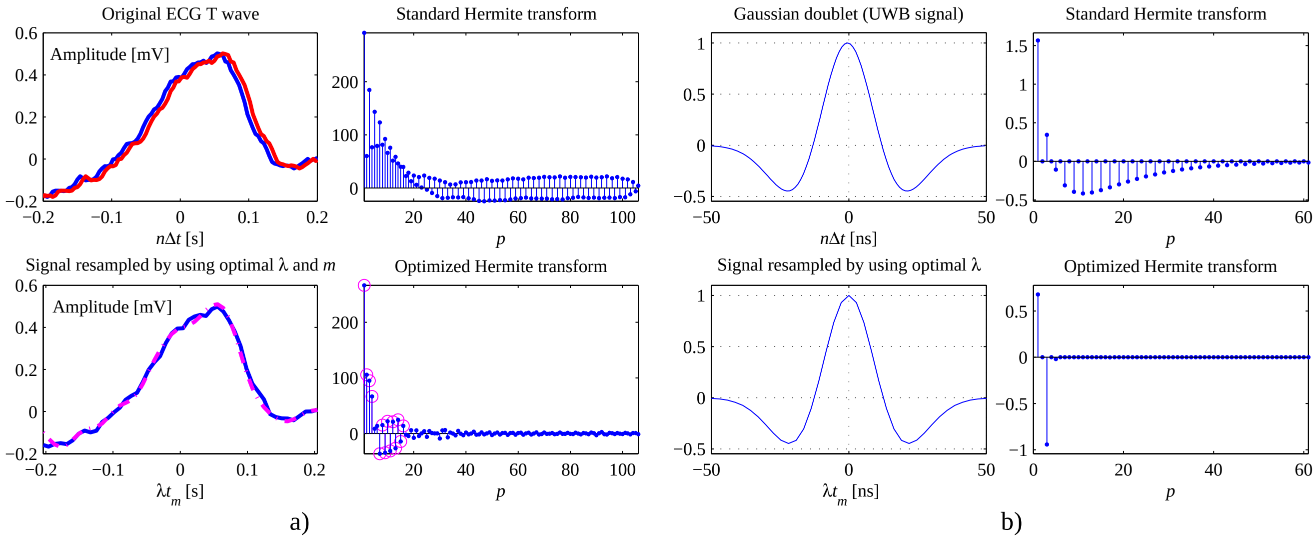

Fig. 5. a) Application to ECG T waves, b) application to the UWB signals

5. Conclusion

An optimization approach for the Hermite transform scaling factor and time-shift is presented. Concentration measure of the transform is employed as the optimization criterion. An iterative algorithm for the scaling factor search is presented. The results are confirmed on both synthetic signal and real ECG signals. The presented theory is applied in the compression of QRS complexes, reducing the average number of coefficients that need to be stored. Finally, it has been shown that the same concept can be also applied to other segments of ECG signal (such as T waves), but also to the UWB signals in communications.

Acknowledgement

This work is supported by the Montenegrin Ministry of Science, project grant: CS-ICT “New ICT Compressive sensing based trends applied to: multimedia, biomedicine and communications” (Grant No. 01-1002).

References

[1] A. Sandryhaila, S. Saba, M. Puschel, J. Kovacevic, Efficient compression of QRS complexes using Hermite expansion, IEEE Trans. Signal Process. 60 (2) (2012) 947–955, doi: 10.1109/TSP.2011.2173336.

[2] A. Sandryhaila, J. Kovacevic, M. Püschel, Compression of QRS complexes using Hermite expansion, in: International Conference on Acoustics, Speech and Signal Process. (ICASSP), IEEE, Prague, 2011, pp. 581–584, doi: 10.1109/ICASSP.2011.5946470.

[3] L. R. L. Conte, R. Merletti, G. V. Sandri, Hermite expansion of compact support waveforms: Applications to myoelectric signals, IEEE Trans. Biomedical Engineering 41 (12) (1994) 1147–1159, doi: 10.1109/10.335863.

[4] M. Brajović, I. Orović, M. Daković, S. Stanković, Gradient-based signal reconstruction algorithm in the Hermite transform domain, Electronics letters 52 (1) (2016) 41-43, doi: 10.1049/el.2015.1700.

[5] P. Laguna, R. Jané, S. Olmos, N. V. Thakor, H. Rix, P. Caminal, Adaptive estimation of QRS complex wave features of ECG signal by the Hermite model, Medical and Biological Engineering and Computing 34 (1) (1996) 58–68, doi: 10.1007/BF02637023

[6] L. Sörnmo, P. O. Börjesson, P. Nygards, O. Pahlm, A method for evaluation of QRS shape features using a mathematical model for the ECG, IEEE Trans. Biomedical Eng. 28 (10) (1981) 713–717, doi: 10.1109/TBME.1981.324666.

[7] M. Lagerholm, C. Peterson, G. Braccini, L. Edenbranhdt, L. Sörnmo, Clustering ECG complexes using Hermite functions and self-organizing maps, IEEE Trans. Biomedical Eng. 47 (7) (2000) 838–848, doi: 10.1109/10.846677.

[8] G. Leibon, D. N. Rockmore, W. Park, R. Taintor, G. S. Chirikjian, A fast Hermite transform, Theoretical Computer Science 409 (2) (2008) 211–228, doi: 10.1016/j.tcs.2008.09.010.

[9] J.-B. Martens, The Hermite transform—Theory, IEEE Trans. Acoustics, Speech, and Signal Process. 38 (9) (1990) 1595–1605, doi: 10.1109/29.60086.

[10] A. I. Rasiah, R. Togneri, Y. Attikiouzel, Modelling 1-D signals using Hermite basis functions, IEE Proc. Vision, Image and Signal Process. 144 (6) (1997) 345–354, doi: 10.1049/ip-vis:19971613.

[11] E. Moya-Albora, B. Escalante-Ramíreza, E. Vallejob, Optical flow estimation in cardiac CT images using the steered Hermite transform, Signal Process.: Image Communication 28 (3) (2013) 267–291, doi: 10.1016/j.image.2012.11.005.

[12] S. Stanković, I. Orović, A. Krylov, The two-dimensional Hermite S-method for high resolution inverse synthetic aperture radar imaging applications, IET Signal Process. 4 (4) (2010) 352–362, doi: 10.1049/iet-spr.2009.0060.

[13] P. Lazaridis, G. Debarge, P. Gallion, Discrete orthogonal Gauss–Hermite transform for optical pulse propagation analysis, J. Opt. Soc. Am. B 20 (7) (2003), 1508–1513, doi: 10.1364/JOSAB.20.001508.

[14] S. Stanković, I. Orović, E. Sejdić, Multimedia signals and systems, Springer - Verlag, New York, 2012, doi: 10.1007/978-1-4614-4208-0.

[15] R. Ma, L. Shi, Z. Huang, Y. Zhou, EMP Signal Reconstruction Using Associated-Hermite Orthogonal Functions, IEEE Trans. on Electromagnetic Compatibility 56 (5) (2014) 1242–1245, doi: 10.1109/TEMC.2014.2312003.

[16] Mengtao Yuan, A. De, T. K. Sarkar, Jinhwan Koh, Baek Ho Jung, Conditions for generation of stable and accurate hybrid TD-FD MoM solutions, IEEE Trans. on Microwave Theory and Techniques 54 (6) (2006) 2552–2563, doi: 10.1109/TMTT.2006.875823.

[17] B. A. Rajoub, An efficient coding algorithm for the compression of ECG signals using the wavelet transform, IEEE Trans. Biomedical Eng. 49 (4) (2002) 355–362, doi: 10.1109/10.991163

[18] N. Boukhennoufa, K. Benmahammed, M. A. Abdi, F. Djeffal, Wavelet-based ECG signals compression using SPIHT technique and VKTP coder, in: 3rd Int. Conf. on Signals, Circuits and Systems (SCS), Medenine, 2009, pp. 1–5, doi: 10.1109/ICSCS.2009.5412584.

[19] S. Olmosa, J. Garcíaa, R. Janéb, P. Lagunaa, ECG signal compression plus noise filtering with truncated orthogonal expansions, Signal Process. 79 (1) (1999) 97–115. doi:10.1016/S0165-1684(99)00083-3.

[20] LJ. Stanković, A measure of some time-frequency distributions concentration, Signal Process. 81 (3) (2001) 621-631, doi: 10.1016/S0165-1684(00)00236-X.

[21] LJ. Stanković, M. Daković, S. Vujović, Adaptive Variable Step Algorithm for Missing Samples Recovery in Sparse Signals, IET Signal Process. 8 (3) (2014) 246–256, doi: 10.1049/iet-spr.2013.0385.

[22] M. Elad, Sparse and Redundant Representations: From Theory to Applications in Signal and Image Processing, Springer, New York 2010.

[23] MIT-BIH ECG Compression Test Database [Online]. http://www.physionet.org/physiobank/database/cdb

[24] M. Abramowitz, I.A. Stegun (eds), Handbook of mathematical functions, Dover Publ., New York, 1992.

[25] W. Gautschi, Orthogonal Polynomials: Computation and Approximation. Oxford Univ. Press, Oxford, U.K., 2004.

[26] Z. Xu, B. Huang, K. Li, On Fourier Interpolation Error for Band-Limited Signals, IEEE Trans. on Signal Process. 57 (6) (2009) 2412–2416, doi: 10.1109/TSP.2009.2016263.

[27] A. Papoulis, Signal analysis, McGraw-Hill, New York, 1977.

[28] T. I. Laakso, V. Valimaki, M. Karjalainen, U. K. Laine, Splitting the unit delay [FIR/all pass filters design], IEEE Signal Process. Magazine 13 (1) (1996) 30–60, doi: 10.1109/79.482137.

[29] M. Z. Win, R. A. Scholtz, Ultra-wide bandwidth time-hopping spread spectrum impulse radio for wireless multiple-access communication, IEEE Trans. on Communications, 48 (4) (2000) 679–691, doi: 10.1109/26.843135.

[30] F. Ramirez-Mireles, On the performance of ultra-wide-band signals in Gaussian noise and dense multipath, IEEE Trans. on Vehicular Technology 50 (1) (2001) 244–249, doi: 10.1109/25.917932.

[31] M. Ghavami, L.B. Michael, R. Kohno, Ultra Wideband Signals and Systems in Communication Engineering, 2nd Edition, Wiley, 2007.